

# Earthquake's Rubble Heaps Volume Evaluation: Expeditious Approach Through Earth Observation and Geomatics Techniques

Sergio Cappucci<sup>(✉)</sup> , Luigi De Cecco, Fabio Gemerei,  
Ludovica Giordano , Lorenzo Moretti, Alessandro Peloso,  
Maurizio Pollino , and Riccardo Scipinotti 

ENEA - Italian National Agency for New Technologies,  
Energy and Sustainable Economic Development, Roma, Italy  
{sergio.cappucci, luigi.dececco, fabio.geremei,  
ludovica.giordano, lorenzo.moretti, alessandro.peloso,  
maurizio.pollino, riccardo.scipinotti}@enea.it

**Abstract.** When an earthquake of a certain magnitude hit a populated zone, a huge amount of data have to be collected in order to address the typical hazard and emergency actions for rescue, assistance, viability, etc. In this paper we concentrate our attention on a particular dataset used to estimate the amount (and location) of rubbles generated by partial or total collapse of buildings/structures, which strongly influences the consequent environmental hazard and reconstruction phase. Despite this information is particularly valuable for optimizing the emergence response, for example by improving the management of their prompt removal, there are not many methods to estimate the amount of the rubbles in terms of volume/weight. Here, a procedure to estimate the volume of rubble heaps through earth observation data and Geomatics techniques is presented and preliminary results discussed.

**Keywords:** Earthquake · Rubbles · Geomatics · LIDAR · Post-emergency management · Emergency Management System COPERNICUS

## 1 Introduction

The central Apennines is one of the most seismically active areas in Italy and Europe. Central Italy is characterized by a rural and mountain landscape with several small ancient villages, teeming with tradition and cultural assets, characterized by poorly engineered buildings and structures.

Generally, the bigger and closer the earthquake, the stronger the shaking. There have been significant earthquakes with extraordinarily modest damage either because they caused little shaking or because the buildings were construct to withstand that level of acceleration on the land surface. In other cases, modest earthquakes have caused considerable damage either because the trembling was locally amplified, or more likely because the structures were poorly engineered. The latter case is what happen in central Italy on the borders of Umbria, Lazio, Abruzzo and Marche regions

on 24 August 2016 when a 6.0-magnitude scale earthquake occurred, followed by thousands of localized aftershocks (more than 60,000 on April 2017), whose some powerful ones (5.3–6.5 magnitude; see Sect. 1.1).

After the rescue activities and beside the typical actions taken to restore the transport and communication networks and to ensure safety and assistance to the local population, a parallel emergency immediately appears to be tackled: the management of the huge amount of rubbles heaps. Their weight is always unknown and their volume has to be estimated in order to plan the best possible management options.

Many studies related to waste management generated by catastrophic events have been conducted by using weight dataset either measured before or after transportation of waste to treatment or recycling plants [1, 2]. But, typically, this evaluation is possible only after a long time from the event.

The volume and variety of disaster waste are often difficult to assess. For the institution in charge of their removal is difficult and risky to rely only on what is possible to observe from the ground perspective, in order to deal with the organisation and management of the necessary actions (e.g., building demolition, rubbles removal [3]). After the 2010 Haiti earthquake, Talbot and Talbot [4] demonstrated the post-event performance of a fast rubble detection algorithm applied at the server, which enhances mono-temporal optical imagery in less than one second/plat, indicating that an end-to-end prototype designed to meet the needs of first responders after disaster is needed.

In our study, requested by the Italian National Civil Protection Department (CPD), we outline a specific and straightforward approach to estimate the rubble heaps volume. The study is mainly based on the LIDAR and Earth Observation (EO) dataset provided by the CPD acquired in the immediate post-event period within the framework of Emergency Management System (EMS) COPERNICUS.

In the Italian disaster management framework, such approach represents an innovative way to deal with post-emergency tasks. Nevertheless, it still needs a massive effort to make it reliable and adoptable by National and Local Authorities as an operative protocol. At the same time, we specify that we do not present or discuss any data related to building stability, earthquake resonance on building or reasons why buildings of different characteristics (e.g., height or construction materials) responded differently during the earthquake. Finally, it is worth highlighting that in some cases apparently undamaged buildings (at time of LIDAR and orthophotos surveys and from the perspective of visual photointerpretation) may have been partially or totally destroyed later on during following aftershocks.

## 1.1 Earthquake Events

The first relevant shock occurred at 3:36 A.M. of August 24<sup>th</sup>, 2016 and had a magnitude of 6.0, with a hypocentre at a depth of 8 km situated along the Valle del Tronto, between the towns of Accumoli (RI) and Arquata del Tronto (AP). Other two powerful earthquakes took place on October 26<sup>th</sup> and 30<sup>th</sup>, 2016 with epicentres in the Umbria-Marche border (the strongest shock, with moment magnitude of 6.5 having its epicentre between the towns of Norcia and Preci). On January 18<sup>th</sup>, 2017 a new

sequence of four strong events (more than magnitude 5 shocks) took place between the towns of L'Aquila Montereale and Capitignano. The earthquakes and aftershocks were felt in most of Central and Northern Italy. The seismic event area is located in a very active seismological part of Central Italy that also includes L'Aquila, where the earthquake of April 6<sup>th</sup>, 2009 caused more than 300 deaths and about 65,000 displaced people. Further back in time, another relevant event happened in Marche and Umbria regions (September 26<sup>th</sup>, 1997). A detailed list of the main earthquake events recently occurred in Central Italy (since August 24<sup>th</sup>, 2016) is retrievable from the INGV (Italian National Institute of Geophysics and Volcanology) website [5].

## 2 Study Area

Immediately after the event, the CPD entrusted Helica Ltd. company (<http://www.helica.it/>) with LIDAR and orthophotos data acquisition over seven - geographically separated - areas hit by the earthquakes (Fig. 1).

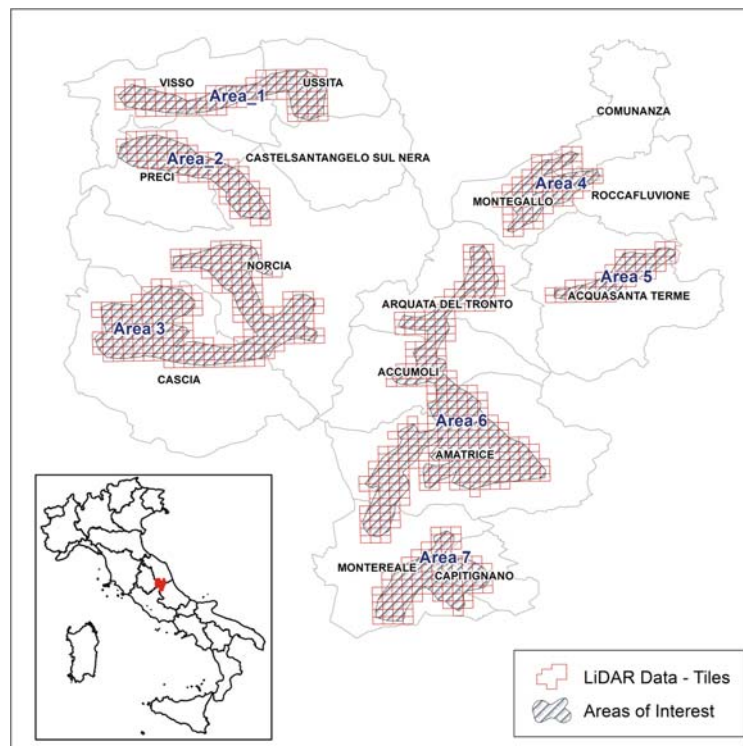


**Fig. 1.** Overview LIDAR surveyed areas (Source: CPD and Helica Ltd.).

### 2.1 Geology

Apennines are affected by a multiphased contraction and extensional tectonics [6]. A fault and thrust system belt, formed by African European continental margins collision during Neogene which result in development of Umbria–Marche northern Apennines and Lazio–Abruzzo Central Apennines [7, 8]. Then, Apennines belt was interested by a post orogenic extension. Such extension is expressed by superficial

faulting [9]. The fault system (N) NW - (S) SE trending and usually 10–30 km long is the uppermost part of a complex normal-oblique system (Fig. 2). Many studies described and quantified the Holocene displacement of faults [10]. In Fig. 3, a simplified geological section show the complex geometric pattern along a WSW-ENE transect [11].

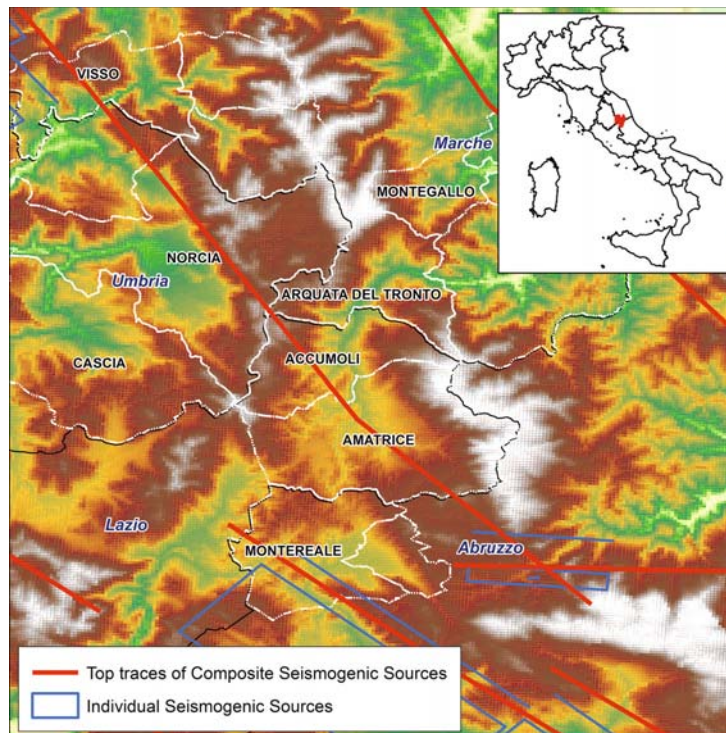


**Fig. 2.** Study area. Seismogenic sources (blue) and some of their top traces (red) are indicated in the areas interested by the first earthquake. (Color figure online)

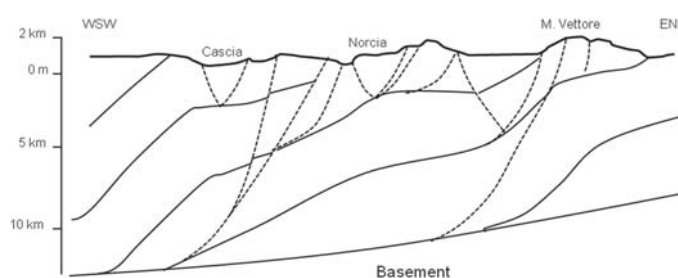


**Fig. 3.** Schematic geological section of the complex geometric pattern WSW-ENE oriented across Norcia-M. Vettore. Modified from [11].

Amatrice and many other villages interested by spread collapses and damaged buildings are predominantly located on ridges and incoherent deposit [12]. This circumstance may have influenced local increase of acceleration, but no data analysis is available at present to prove such hypothesis. The two most essential variables influencing earthquake damages are (1) the intensity of ground shaking caused by the event tied with (2) the quality of the engineering of structures in the area. The level of

trembling itself is strongly influenced by the proximity of the earthquake source to the affected region and the types of rocks (mostly those at or close to the land surface) that seismic waves pass through during their propagation.

### 3 Data and Methods

#### 3.1 Dataset

The core dataset is made up of:

1. LIDAR Point Clouds (2016, *post-event* flight- provided by CPD);
2. 1 m-pixel Digital Terrain Model (DTM; derived from LIDAR data acquired during 2016 flight, hereinafter indicated as  $DTM_{post}$ );
3. 1 m-pixel Digital Surface Model (DSM; derived from LIDAR data acquired during 2016 flight, hereinafter indicated as  $DSM_{post}$ );
4. RGB orthophotos (15 cm ground spatial resolution, 2016 flight);
5. LIDAR Point Clouds (2008-2012 acquisition flights, *pre-event*, provided<sup>1</sup> by the Ministry of the Environment and Protection of Land and Sea of Italy (MATTM) and made available through the Italian National Geoportal);
6. 1 m-pixel DTM (derived from above mentioned 2008–2012 LIDAR flights, hereinafter indicated as  $DTM_{pre}$ );
7. 1 m-pixel DSM (derived from above mentioned 2008-2012 LIDAR flights, hereinafter indicated as  $DSM_{pre}$ );
8. Damaged/collapsed buildings: delimitation and classification (provided by Copernicus Emergency Management Service [13]).

As listed above, two LIDAR datasets were available: one acquired few days after the August 24<sup>th</sup> earthquake and the other referred to some years before the event (and available only for a portion of the investigated areas). All the DSM and DTM data, in raster format, pre and post-earthquake, are at the same spatial resolution: 1 pixel per square meter. In the following Section, different approaches are presented, using either only post-earthquake data or exploiting the pre-existing DSM and DTM data, too.

Specifically, data listed from 1 to 4 were provided by the CPD: in particular, these data were acquired by the Helica Ltd. by means of a  $\sim 1000$  m altitude flights, during which the RGB orthophotos were acquired too. Helica pre-processed the 10 dots/m<sup>2</sup> LIDAR dataset (about 9 million points clouds) and generated the DSM and DTM layers, by mosaic them in 892 tiles ( $700 \times 700$  m each). In Fig. 4, an example of different data layers available for one of the hit zones is reported.

Data listed from 5 to 7 were provided by the MATTM and refer to a pre-earthquake status as data were acquired during flights occurred between 2008 and 2012. Elevations data are in this case orthometric heights (measured above the geoid). However, it has to be highlighted that these data didn't cover the whole hit zones, since they were acquired for different purpose.

<sup>1</sup> <http://www.pcn.minambiente.it/geoportal/catalog/search/resource/details.page?uuid=%7BB8A39D4E-D7DF-4621-9318-4EEE3B1511CF%7D> (Source: Italian National Geoportal).

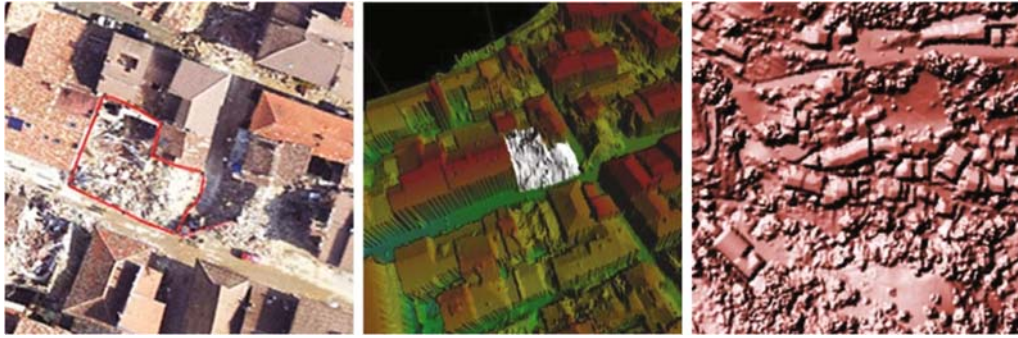


**Fig. 4.** Orthophoto, post-event LIDAR Point Cloud (3-D rendering) and DSM extracted from LIDAR data.

The geodetic system used is ETRS89, implementing the realization ETRF2000 for 2008-12 LIDAR dataset. The coordinate system is UTM-WGS84-ETRF2000 Zone 33, according to the reference system of map cartography used in this part of Italy. It is worth underlining that this dataset is characterized by ellipsoidal heights, since it is not possible to transform them into orthometric heights until the new after-shock reference point's height will be upgraded by the *Istituto Geografico Militare Italiano* (IGMI). In some case, Google street view data (e.g. buildings and streets characteristics such as building's elevation, street's path tendency) as well as data provided by Social Network/other web sources were considered - where available - as ancillary information (Fig. 5). The damaged buildings map (Fig. 10b) derives from Copernicus EMS (Activation EMRS177<sup>2</sup>).



**Fig. 5.** A building before the earthquake and the same collapsed building pointed out in the orthophotos acquired after the event (blue line indicates the field of view). (Color figure online)

### 3.2 Methodology

In order to store and share all data among the multiple users, an HW/SW architecture based on the specific Spatial Data Infrastructure (SDI), already available and running in the ENEA [14, 15], was exploited (Fig. 6). The SDI was developed in a FOSS4G (Free

<sup>2</sup> <http://emergency.copernicus.eu/mapping/list-of-components/EMSR177>.

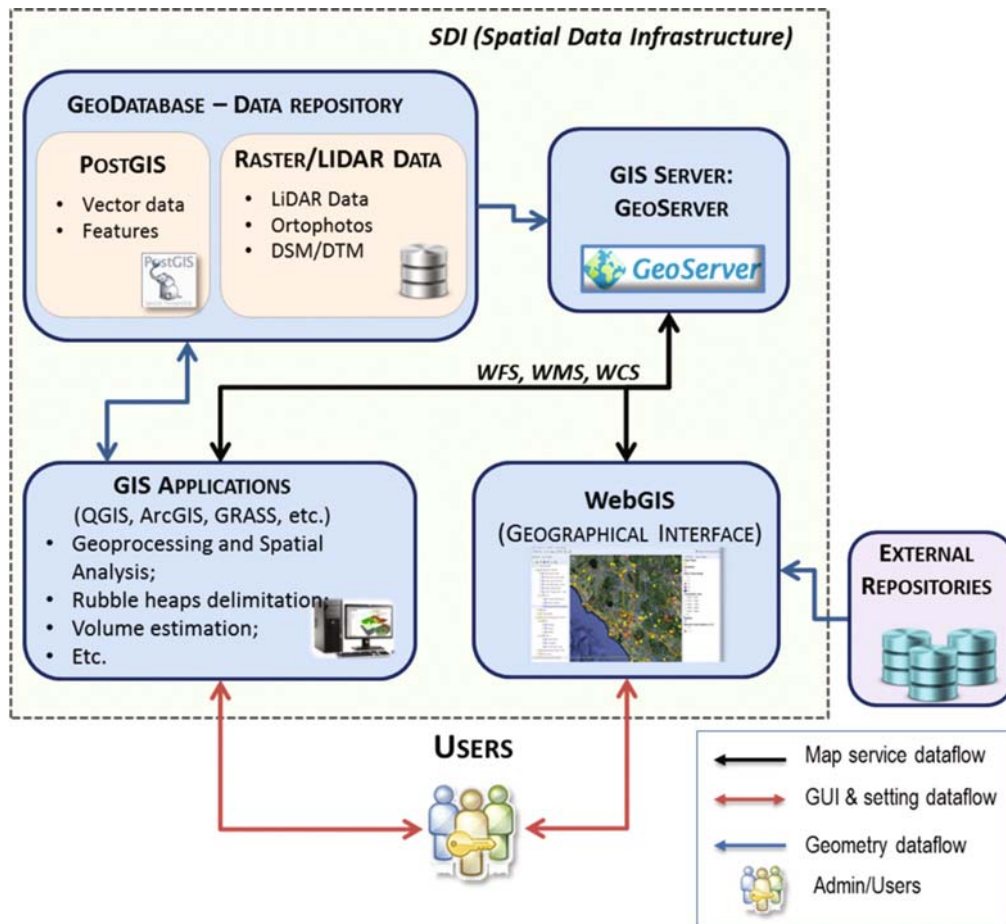


Fig. 6. HW/SW architecture of the exploited SDI

and Open Source Software for Geospatial) environment [16, 17]: a PostGIS-based GeoDatabase (GeoDB) [18] for data storage and management was realized. The GeoDB can be directly accessed by means of different desktop GIS software suites (e.g., QGIS). Then, by means of the server stratum, composed by GeoServer [19], data can be accessed via web by means of OGC standards (WMS, WFS and WCS services). Moreover, a restricted WebGIS application (accessible using appropriate credentials) and developed in the GeoPlatform environment (a free/open source suite developed by geoSDI [20]), has been implemented [21]. A specific layout, thus, was created so as to further support our mapping activities (Fig. 7).

In order to take into account different issues, typical of such a kind of emergency situations (e.g., the availability/lack of data, the specific needs of stakeholders, etc.), and to tackle appropriately them, two different methodologies, indicated as M1 and M2, respectively, were conceived and applied. The first one (M1) has been defined in order to be adopted in case of no pre-event data (e.g. LIDAR) are available and/or exploitable; the second one (M2) is based on the availability and exploitability of previously acquired (pre-event) LIDAR data (i.e.,  $DSM_{pre}$ ,  $DTM_{pre}$ ).

Whatever the methods used, the following assumptions were made on rubble heaps volume evaluation:

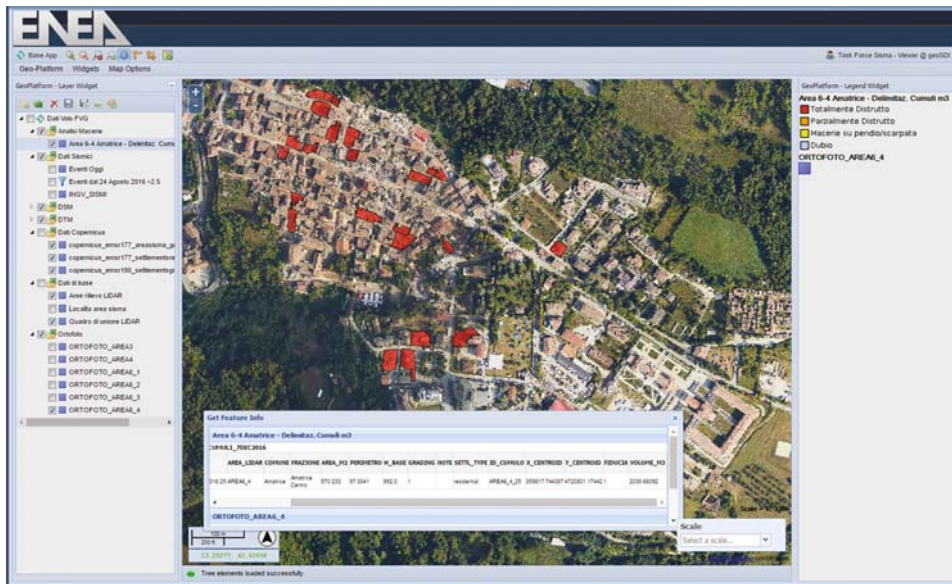


Fig. 7. WebGIS application interface

- volume is referred to the situation related to the LIDAR data acquisition time, as buildings collapsed at a later time are not considered in our analysis;
- Ground Control Points (coming from in-situ check) were not used to calculate the actual absolute heights, even if during the earthquake a significant variation in elevation has been recorded, reaching 18 cm in some points. New official reference heights will be provided by the Institution in charge (IGMI in this case) when emergency will be over;
- volume assessment was carried-out without considering the void ratio, which can be extremely variable as many ruins are composed by a multiple continuous and discontinuous wreckage of different materials (bricks, tiles, reinforced concrete columns and curbs mixed to fragments of metals, wood, home appliances and other bulky wastes).

Additionally, only in M1, the following assumption was done, too:

- variation of terrain elevation underneath the rubble heap perimeter was not considered. It means that a flat horizontal surface (points laying at a constant elevation) was always considered as the base of the rubble heap's volume.

*Method 1.* The implemented methodological approach, outlined in Fig. 8, is structured into the following steps:

1. The collapsed buildings (rubble heaps perimeters) were delimited by means of visual photo-interpretation, taking advantage of orthophotos' high resolution (15 cm) as well as using the already available Copernicus EMS data [13]. The polygons (P) were traced considering the displacement caused by the oblique photo acquisition (e.g., by integrating the  $DTM_{post}$  and  $DSM_{post}$  in the assessment). Wherever possible, i.e. when a single building was effectively recognizable as a well-defined single structure, a unique rubble heap was digitized for each single

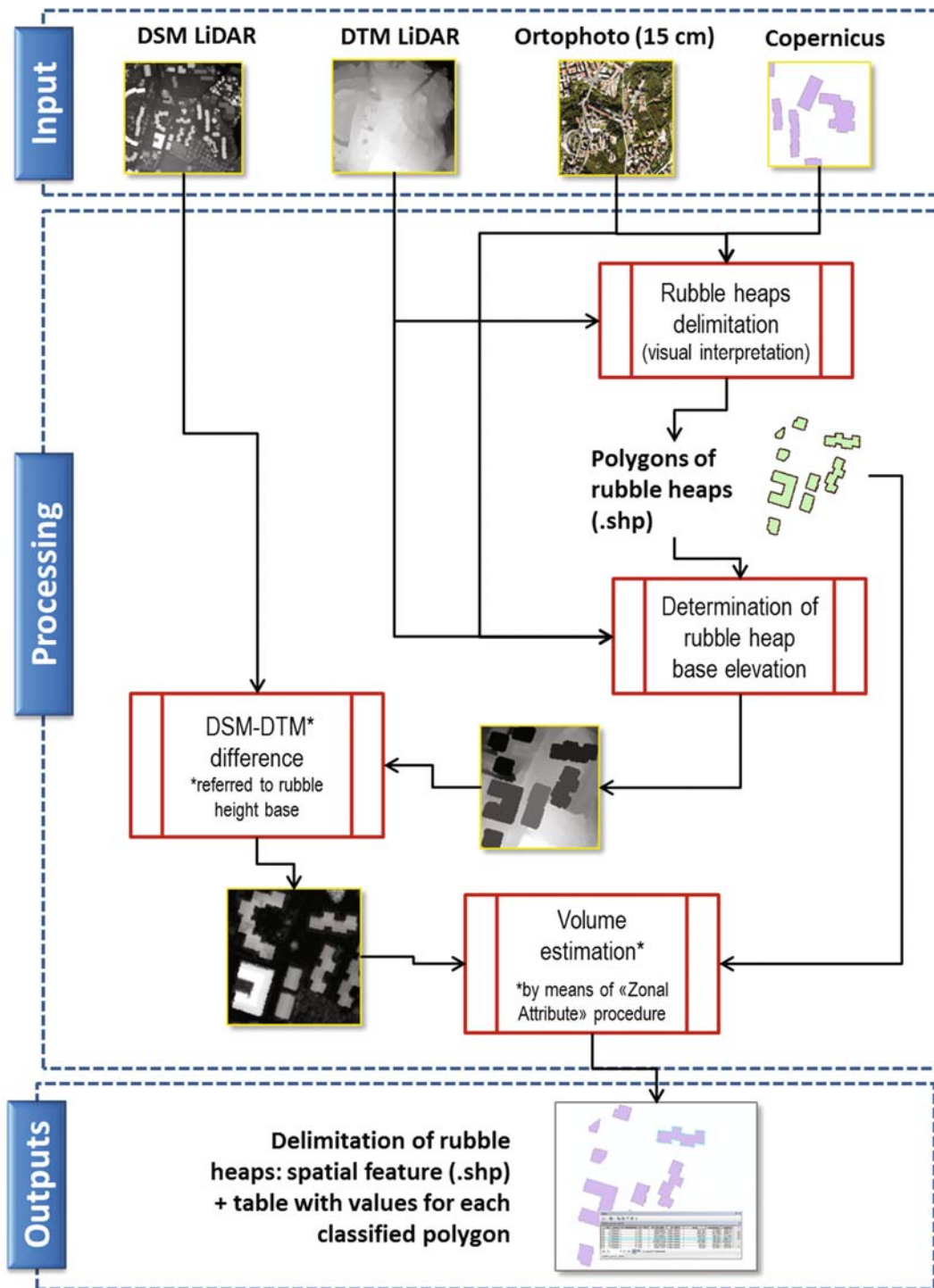


**Fig. 8.** Flow chart of the methodological approach pursued.

building; a pooled polygon referring to a group of (not distinguishable) buildings was sketched otherwise.

2. A suitable classification of “level of damage” has been reported, by assigning specific codes to each polygon: (1) “totally collapsed”; (2) “partially collapsed”, (3) “rubbles piled over a slope”; (4) “uncertainty in defining the level of damage”.

3. In addition, a classification of building's typology was performed (assigning a specific class, e.g. "religious", "residential", "educational", "medical", etc.), to each polygon, supported by Copernicus EMS data, as well as other web sources like Google Maps.
4. To each polygon, the building's base elevation value (B) was assigned: it was derived from the  $DTM_{post}$  in correspondence of a visible point (e.g., portion of the surrounding streets free of rubbles), identified close to the considered building block/rubble. In case of a significant slope of the streets contiguous to the building block, the minimum altitude value among different possible points nearby the area of interest was selected, to not underestimate the actual elevation of rubble heaps (Fig. 9).



**Fig. 9.** Example of building's base height retrieving. The elevation is estimated from the lower (visible) point adjacent the rubble heap. For instance, in case 2 the lower elevation (right side) is selected.

5. On the basis of the previously described steps, the volume of a single rubble heap can be estimated as the solid (3-D space) included between the flat horizontal polygon, i.e. the bottom surface (B) represented by the building's foundation developing at a constant altitude (selected  $DTM_{post}$  value), and the upper uneven surface represented by the  $DSM_{post}$  values over the polygonal area itself. So, the volume is assessed through the difference between the  $DSM_{post}$  and the selected  $DTM_{post}$  value (constant altitude B) over the area identified by the heap's perimeter, as expressed by the formula (1):

$$V_{M1} = B \cdot \sum_{k=0}^n \binom{n}{k} h^{DSM_{post}} \quad [m^3] \quad (1)$$

where B is the elevation value of the rubble heap's base and h is the elevation value (in m) extracted from the  $DSM_{post}$  for each pixel, n = number of pixel. Volume values are expressed in  $m^3$ .

This calculation was carried out in GIS environment by means of the ERDAS Imagine "zonal attribute" function<sup>3</sup>, which allows to assign the calculated volume value

<sup>3</sup> Zonal Statistics To Polygon Attributes: this ERDAS Imagine (by Hexagon Geospatial) operator extracts the zonal statistics of the background image of a vector feature layer and save them as vector attributes.

as an attribute of the corresponding GIS polygon representing the rubble heap (in shapefile format).

*Method 2.* Method 2 follows the same steps 1 and 2 of M1 but different step 3, since the assignment of the elevation values of rubble’s base is not manually performed. Rather, the base values are automatically extracted by the pre-event DTM<sub>pre</sub>, which can be assumed as the bottom surface.

Therefore, in M2 processing chain, the volume calculation is directly obtained by the difference in elevation between post-event DSM<sub>post</sub> and pre-event (DTM<sub>pre</sub> over the rubbles’ perimeter (step 3), as described in Eq. (2):

$$V_{M2} = \sum_{k=0}^n \binom{n}{k} h^{DSM_{post}} - \sum_{k=0}^n \binom{n}{k} h^{DTM_{pre}} \quad [m^3] \quad (2)$$

However, particular attention is needed in order to make the two datasets (post- and pre-event) consistent with each other in case of differences in the absolute elevation reference system among them, and the variation in height, which can occur over some of the areas hit by earthquakes.

Ultimately, we investigated an additional approach limited to the exploitation of LIDAR data after and before the earthquake, thus without using any orthophotos and the manual extraction of height values from DTM. In fact, the raster resulting from the difference DSM<sub>post</sub> – DSM<sub>pre</sub> may provide an overview and a rapid assessment of collapsed areas, ideally returning a null value wherever nothing happened, negative values where buildings collapsed and positive values where rubble heaps piled up over previous clear area (e.g., streets, courtyards, etc.). We do not have obtained consolidated results yet and we can argue that the idea deserves to be further developed. However interesting preliminary results were obtained at least in terms of automatic location (and geometrically definition) of rubbles (fair agreement with results manually obtained in step 1 (in M1/M2).

## 4 Results

The present study shows the possible results, in terms of rubble’s volume estimation, which can be provided in a rather short time starting from LIDAR and orthophotos datasets. In particular, a total of about 15,000 m<sup>2</sup> of rubble heaps were identified and outlined in the area of Amatrice, corresponding to a total volume of about 75,000 m<sup>3</sup>. In Table 1 a summary of the total amount of rubble volumes assessed by using the two

**Table 1.** Estimated rubble heaps volume in Amatrice area

Municipality	Settlement type	Volume M1 (m <sup>3</sup> )	Volume M2 (m <sup>3</sup> )
Amatrice	residential	54,827.1	56,021.8
	religious	18,112.3	19,655.4
Total vol. (residential + religious)		73,826.0	75,764.0

different methodologies (as described in Sect. 3.2) is reported. It is worth highlighting that those heaps are the majority but not the total amount of rubbles in this area, as this is an ongoing research (aiming at testing the approach) and thus only the preliminary results are here presented.

As an example, selected perimeters of rubble heaps identified in Amatrice's area are reported in Fig. 10a. The same polygons are classified according to the level of damage (Fig. 10b), to the settlement typologies (Fig. 10c) and to the estimated volume of each single rubble heap (Fig. 10d): this helps to understand the potential applicability of the results obtained in the frame of our research.

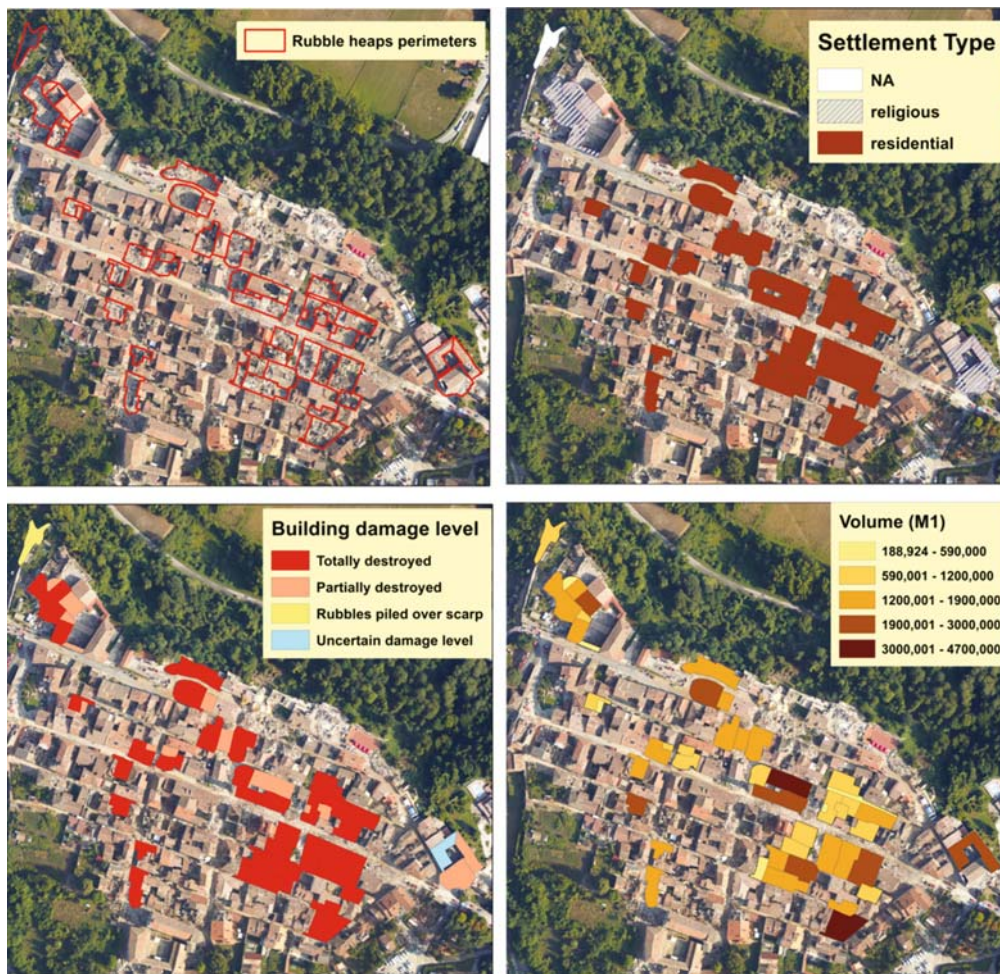


**Fig. 10.** Polygons: (a) representing rubble heaps delimitation in Amatrice; (b) classified according to the level of damage; (c) referring to the settlement typologies (residential, religious, etc.); (d) volume values ( $m^3$ ).

In Fig. 11 the raster images whose values represent the difference between the  $DSM_{post}$  and  $DSM_{pre}$  are reported. This additional approach offers a viable solution only in case a pre-existing  $DSM_{pre}$  is available in the affected area: those datasets may also be utilized when orthophotos are not (or not yet) available.

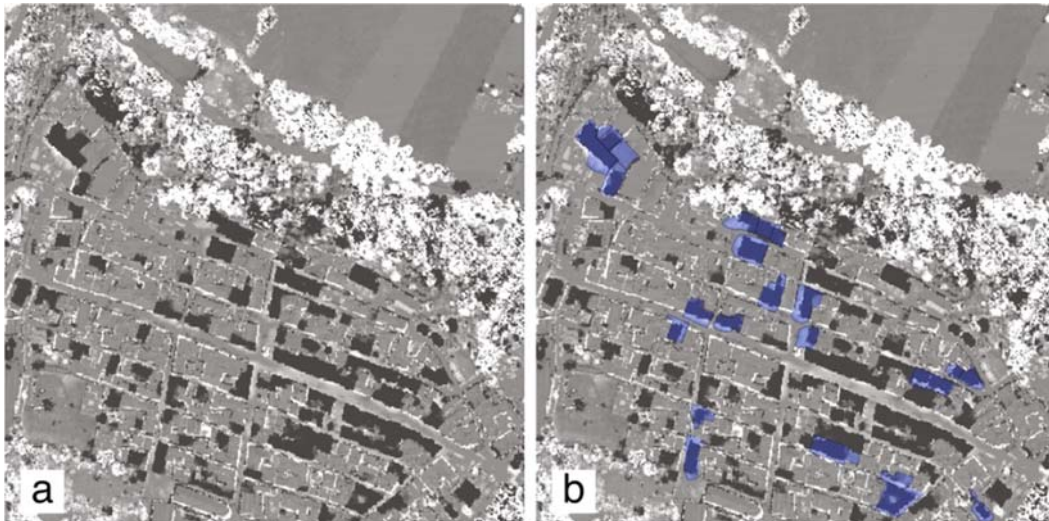


**Fig. 11.** Raster images resulting by the difference ( $DSM_{\text{post}} - DSM_{\text{pre}}$ ): (a) darker areas indicate the collapsed buildings; (b) blue polygons are the automatically selected areas for rubbles volume estimation. (Color figure online)

## 5 Discussion and Conclusions

For each rubble heaps it was possible to delineate the perimeter (that is the surface extension) with a high degree of accuracy, thanks to the high resolution of orthophotos obtained immediately after the earthquake event. In order to support specific management needs, such as the restoration of a particular site, viability, etc. for each polygon (rubble heap) a corresponding address was associated, too. Tracing of the polygons (rubble heap) is a time consuming task especially if the aim is to associate each rubble heaps to a single source (building generating the rubble). To this aim we tried to subdivide into multiple polygons what was actually a single heap. However, especially in areas interested by many contiguous collapsed building, it was not easy, sometimes even not feasible, to retrieve the exact rubble-building correspondence.

In other cases, some uncertainty remains about the actual grade of a building's damage: for example, the combination of rubbles and an apparently intact building leaves doubts about the real stability of the structure and the consequent prediction about the management of such specific situation (i.e. building to be demolished or restored).

In the present study, we would like to stress that different methods may be applied depending on the available resources (i.e. time/budget/data).

Therefore, two methodologies (M1 and M2, see Sect. 3.2) have been implemented in order to provide effective support to the CPD operators and to cooperate with the existing Copernicus EMS service. M1 uses a single, consistent set of data (collected immediately after the event) whereas the other, M2, needs pre-existing LIDAR data (specifically DTM) to be available and the consequent adjustment to be performed in order to obtain consistent datasets.

As described in the Results Section, in M1 a flat surface is considered as the bottom side of rubble's volume, whose z-position (height) needs to be manually retrieved by

operators (which have to look for a rubble-free point as near as possible to the rubble itself). In some cases, it was not so easy to find a heap-free point to retrieve the building's base height due to the ruins covering all the surrounding streets. In the second method (M2), the elevations are automatically derived from the pre-existent  $DTM_{pre}$ , hence overcoming such a drawback, though adjustment are likely necessary in order to make the two datasets (pre- and post-event) coherent one with the other. The presence of the rubble heaps themselves can also interfere with the production of the DTM from LIDAR data, leading to less reliable DTM ( $DTM_{post}$ ) values (resulting in a virtual intermediate value between the actual DTM and DSM). Data acquired by LIDAR surveys, indeed, are laser pulses returning to the sensor and measuring in this way the distance to a target. Therefore, by using the flight parameters these data can be easily converted into DSM data. The DTM is instead derived by DSM through a complex algorithm that strongly depends on the slope of the object protruding out the ground, such as houses, trees, people, cars, etc., in order to “subtract” them and retrieve the underlying terrain. For that reason, when the acquisition is performed in a “normal” situation and not after a catastrophic event, the elevation of the terrain (i.e. the resulting DTM) is very accurate and reliable since there are no errors due to rubbles and/or scattered debris. On the contrary, such debris (commonly present after an earthquake) can be processed as ground level elevation in some spot (see Fig. 12) and some discrepancies can be found comparing the pre-earthquake  $DTM_{pre}$  with the post-earthquake  $DTM_{post}$ .

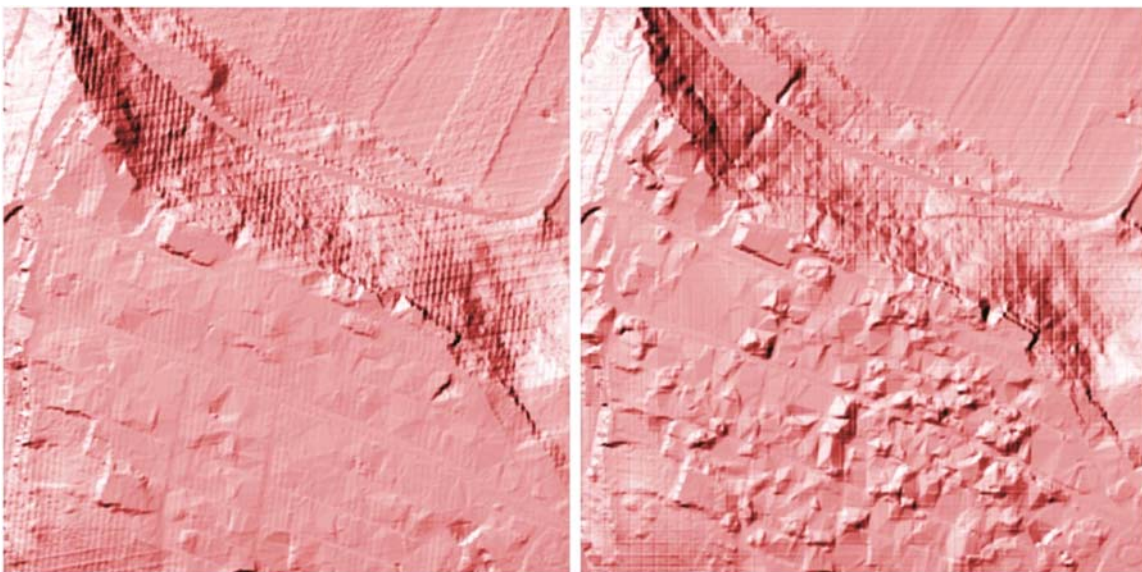


**Fig. 12.** Amatrice centre. On the left, DTM before earthquake (LIDAR flight 2008–2012); on the right DTM after Earthquake 1 (LIDAR flight 2016)

In general, we can argue that whether to use the first or the second proposed methodology (M1 or M2) depends more on the specific case (data, time, skilled manpower available) as well as on the requested result's accuracy. Despite the total volume is basically comparable, as the overall percentage difference is within 2,6%, specific differences, up to 50% in volume, can be found when single rubble heaps are

compared. In fact, significant different results were obtained utilizing the two approaches on small hotspots of collapsed buildings, however weight/volume comparison is still an ongoing challenging activity. For an assessment of the weight must be taken into account some parameters not yet known in the current state and linked to each construction, such as the type of material used, the number of floors and also the housing presence [22, 23].

Clearly, the bigger the surface extension of a rubble, the higher the influence of using a single elevation as the base of the rubble, especially if the actual base is a significantly sloping or uneven surface (e.g., typically along streets). In this case it is better to limit the polygon size at minimum extension with a relevant increase in time consuming processing chain. A specific discussion is needed for when pre and post LIDAR datasets are available. The M2 procedure, using only post event LIDAR dataset, certainly offers a faster procedure to locate the area characterized by buildings' collapses and rubble heaps, along with their volume's estimates. The M1 procedure shows the advantage to consider also differences in landscape that may be occurred between the different data acquisitions.

In fact, the time-span between the two LIDAR datasets can reach more than a few years (in this case 2016 versus 2008–2012), possibly resulting in new housing, roads, changing in vegetation, etc. Such change in detection are not a direct consequence of the earthquake, but only the common dynamics of territories [24] or the emerging issue of urban sprawl [25], which need to be accounted for in some way. It is a challenge we are going to tackle in the future developments of our approach, indeed.

It is worth noting that changes referring to the removal and displacement of debris, collapses or demolition occurred after the date of the survey (post-event dataset) and hence not accounted for in the dataset provided by the National and Local Authorities were not taken into account in the present study.

Ultimately, preliminary results are showing an interesting correspondence between the geology of the area, the level of damages and the volume of the identified rubble heaps which will hopefully produce a research development.

We finally would like to stress the fact that the possibility to use the Copernicus EMS has been vital for the success of our research. Following the European Flood Awareness System (EFAS [26]) and European Forest Fire Information System (EFFIS [27]) we hope that a GIS-based Web-application that provides near real-time and historical information on buildings will be considered by the European Commission (EC) and that the acquisition of LIDAR data will be constantly carried out in order to cover the entire territory at European level.

**Acknowledgments.** The present research has been funded by ENEA and requested by DPC. EO data were provided under COPERNICUS by European Union and ESA. Thanks to Eng. F. Campopiano, P. Marsan and P. Pagliara of National Civil Protection for the fruitful discussion and suggestions and to all staff involved during the emergency action. ENEA is not responsible for any use, even partial, of the contents of this document by third parties and any damage caused to third parties resulting from its use. The data contained in this document is the property of ENEA.

## References

1. United States Environmental Protection Agency: Household Hazardous Waste Management: A Manual for One-Day Community Collection Programs. EPA530-R-92-026, Washington, D.C., August 1993
2. Lund, H.F.: Household Hazardous Wastes. The McGraw-Hill Recycling Handbook (1993)
3. Memon, M.A.: Disaster waste recovery and utilization in developing countries-Learning from earthquakes in Nepal. In: 15th Asian Regional Conference on Soil Mechanics and Geotechnical Engineering, ARC 2015: New Innovations and Sustainability, pp. 143–147 (2015)
4. Talbot, B.G., Talbot, L.M.: Fast-responder: Mobile access to remote sensing for disaster response. *Photogramm. Eng. Remote Sens.* **79**(10), 945–954 (2013)
5. Amatrice, Norcia, Visso Seismic Sequence, INGV. <http://terremoti.ingv.it/it/ultimi-eventi/1023-sequenza-sismica-in-italia-centrale-aggiornamenti.html>. Last access: 28 Mar 2017. (In Italian)
6. Pizzi, A., Galadini, F.: Pre-existing cross-structures and active fault segmentation in the northern-central Apennines (Italy). *Tectonophysics* **476**, 304–319 (2009). doi:[10.1016/j.tecto.2009.03.018](https://doi.org/10.1016/j.tecto.2009.03.018)
7. Coltorti, M., Farabollini, P.: Quaternary evolution of the Castelluccio di Norcia Basin (Umbria-Marchean Apennines, Italy). *Il Quaternario* **8**, 149–166 (1995)
8. King, G.C.P.: Speculations on the geometry of the initiation and termination processes of earthquake rupture and its relation to morphology and geological structure. *Pure Appl. Geophys.* **124**(3), 567–585 (1986)
9. Hernandez, B., Cocco, M., Cotton, F., Stramondo, S., Scotti, O., Courboux, F., Campillo, M.: Rupture history of the 1997 Umbria-Marche (Central Italy) main shocks from the inversion of GPS, DInSAR and near field strong motion data. *Ann. Geophys.* **47**, 1355–1376 (2004)
10. Valensise, G., Pantosti, D.: The investigation of potential earthquake sources in peninsular Italy: a review. *J. Seismol.*, 5287–5306 (2001)
11. Calamita, F., Pizzi, A.: Tettonica quaternaria nella dorsal appenninica umbro-marchigiana e bacini intrappenninici associate. *Studi Geologici Camerti*, SI, 17–25 (1992)
12. Cacciuni, A., Centamore, E., Di Stefano, R., Dramis, F.: Evoluzione morfotettonica della conca di Amatrice. *Studi Geologici Camerti* **2**, 95–100 (1995)
13. Copernicus Emergency Management Service (EMS). <http://emergency.copernicus.eu/>
14. Pollino, M., Modica, G.: Free web mapping tools to characterize landscape dynamics and to favor e-participation computational science and its applications. In: Murgante, B., et al. (eds.) ICCSA 2013, LNCS 7973, Part III, 566–581. Springer, Heidelberg (2013)
15. Modica, G., Pollino, M., Lanucara, S., Porta, L., Pellicone, G., Fazio, S., Fichera, C.R.: Land suitability evaluation for agro-forestry: definition of a web-based multi-criteria spatial decision support system (MC-SDSS): preliminary results. In: Gervasi, O., et al. (eds.) ICCSA 2016. LNCS, vol. 9788, pp. 399–413. Springer, Cham (2016). doi:[10.1007/978-3-319-42111-7\\_31](https://doi.org/10.1007/978-3-319-42111-7_31)
16. Steiniger, S., Hunter, A.J.S.: Free and open source GIS software for building a spatial data infrastructure. In: Bocher, E., Neteler, M. (eds.) *Geospatial Free and Open Source Software in the 21st Century*, pp. 247–261. Springer, Heidelberg (2012)
17. Modica, G., Laudari, L., Barreca, F., Fichera, C.R.: A GIS-MCDA based model for the suitability evaluation of traditional grape varieties: the case-study of ‘mantonico’ grape (Calabria, Italy). *IJAEIS* **5**(3), 1–16 (2014)
18. PostgreSQL with PostGIS extension. <http://postgis.net>

19. Geoserver. <http://geoserver.org/>
20. GeoPlatform by geoSDI. <https://github.com/geosdi/geo-platform>
21. Pollino, M., Caiaffa, E., Carillo, A., Porta, L., Sannino, G.: Wave energy potential in the mediterranean sea: design and development of DSS-WebGIS “waves energy”. In: Gervasi, O., Murgante, B., Misra, S., Gavrilova, Marina L., Rocha, A.M.A.C., Torre, C., Taniar, D., Apduhan, B.O. (eds.) ICCSA 2015. LNCS, vol. 9157, pp. 495–510. Springer, Cham (2015). doi:[10.1007/978-3-319-21470-2\\_36](https://doi.org/10.1007/978-3-319-21470-2_36)
22. CNR-ITC, C.N.VV.FF.: Sisma Abruzzo 6 Aprile 2009 - Stima quantificazione macerie, Activity Report (2010). (In Italian)
23. Marghella, G., Marzo, A., Moretti, L., Indirli, M.: Uso del GIS per il Piano di Ricostruzione di Arsita (TE). In: ANIDIS 2013 – XV Convegno (2013). (In Italian)
24. Modica, G., Zoccali, P., Fazio, S.: The e-participation in tranquillity areas identification as a key factor for sustainable landscape planning. In: Murgante, B., Misra, S., Carlini, M., Torre, C.M., Nguyen, H.-Q., Taniar, D., Apduhan, B.O., Gervasi, O. (eds.) ICCSA 2013. LNCS, vol. 7973, pp. 550–565. Springer, Heidelberg (2013). doi:[10.1007/978-3-642-39646-5\\_40](https://doi.org/10.1007/978-3-642-39646-5_40)
25. Fichera, C.R., Modica, G., Pollino, M.: Land Cover classification and change-detection analysis using multi-temporal remote sensed imagery and landscape metrics. *Eur. J. Remote Sens.* **45**, 1–18 (2012)
26. European Flood Awareness System (EFAS). <https://www.efas.eu/>
27. European Forest Fire Information System (EFFIS). <http://effis.jrc.ec.europa.eu/>